

Algorithm to Generate Target for Anti-Lock Braking System using Wheel Power

Ehsan Arasteh^{1*}, Francis Assadian², Louis Filipozzi¹

¹ Ph.D. student at UC Davis, Department of Mechanical and Aerospace Engineering, USA.

² Professor at UC Davis, Department of Mechanical and Aerospace Engineering, USA.

***Corresponding author:** Ehsan Arasteh. Ph.D. student at UC Davis, Department of Mechanical and Aerospace Engineering, USA.

Received Date: May 22, 2020; **Accepted Date:** June 25, 2020; **Published Date:** July 03, 2020

Citation: Arasteh E., Assadian F., Filipozzi L. (2020) Algorithm to Generate Target for Anti-Lock Braking System using Wheel Power. Journal of Mechanical and Aerospace Engineering, 2(1); Doi:10.31579/jmae.2020/002

Copyright: ©2020 Ehsan Arasteh, This is an open-access article distributed under the terms of the Creative Commons Attribution License, which permits unrestricted use, distribution, and reproduction in any medium, provided the original author and source are credited.

Abstract

This paper discusses creating a suitable reference for the Anti-Lock Braking (ABS) control system that maximizes power recovery or dissipation of the brake system. Current anti-lock brake systems implement a finite-state method algorithm to respond to the wheel longitudinal slip by keeping the slip at the given target to maximize braking force. Variables in the logic can include wheel-speed measured from sensors, brake target slip which is estimated by the Electronic Control Unit (ECU), reference speed, which is also estimated, and vehicle acceleration/deceleration. Angular acceleration and calculated actual wheel slip are used as indicators of the wheel's state of motion. To find the maximum braking force, a typical ABS over-brakes such that the tire longitudinal force exceeds its maximum value and therefore, the wheel starts locking up. The ABS then adjusts by under-braking, and repeats this cycle to keep the tire longitudinal force around its maximum. This paper uses the power absorbed by the wheel to find the maximum power dissipated. Using this strategy, the ABS utilizes a continuous control strategy and can better approximate the maximum brake force without the cyclic method that has been used in the conventional ABS. In addition to maximizing the brake force as a result of this approach, driver comfort also increases due to the continuous control vs. on/off (cyclic) control during an ABS event. The paper discusses theoretical aspects of the problem, and software simulation using MATLAB and Simulink.

Keywords: algorithm; anti-lock braking system; wheel power; electronic control unit (ECU); brake force

Introduction

Current anti-lock brake systems implement a finite-state method algorithm to respond to the wheel longitudinal slip by keeping the slip at the given target to maximize braking force. Variables in the logic can include wheel-speed measured from sensors, brake target slip which is estimated by the Electronic Control Unit (ECU), reference speed, which is also estimated, and vehicle acceleration/deceleration. Angular acceleration and calculated actual wheel slip are used as indicators of the wheel's state of motion. Current continuous control methods focus on nonlinear control techniques such as sliding mode to keep the vehicle's slip at a desired value [1] [2] [3]. Such techniques are often not intuitive, hard to tune and require a lot of computational power to be implemented on the production vehicle.

To find the maximum braking force, a typical ABS over-brakes such that the tire longitudinal force exceeds its maximum value and therefore, the wheel starts locking up. The ABS then adjusts by under-braking, and repeats this cycle to keep the tire longitudinal force around its maximum.

In this paper, we use the one-wheel vehicle model to derive a unique control strategy for the control of a vehicle ABS, using the power absorbed by the wheel to find the maximum power dissipated. Using this strategy, the ABS utilizes continuous control and can better approximate the maximum brake force without the cyclic method that has been used in the conventional ABS. In addition to maximizing the brake force as a result of this approach, driver comfort also increases due to the continuous control vs. on/off (cyclic) control during an ABS event.

The first part of the paper consists of modeling the system. Then, using the dynamics equations of the model, we will lay the groundwork of the use of dissipated power in the context of ABS continuous control. The paper then continues with the simulation results (done in MATLAB and Simulink) and follows with the discussion of the results.

Vehicle and Brake model

Figure 1 shows a single wheel tire and all the forces, moments and velocities while braking. This simple model is chosen for the purpose of initial results on the ABS algorithm proposed in this paper. [4].

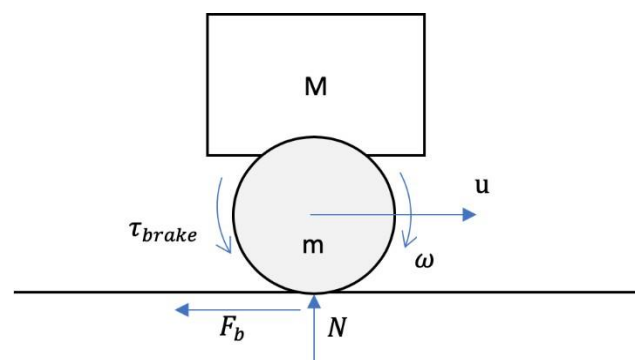


Figure 1: Schematic of forces and torques on the wheel

Equations 1 and 2 describe the dynamic equations for this single wheel tire model.

$$J_w \dot{\omega}_w = F_b R_w - \tau_b \tag{1}$$

$$M \dot{u} = -F_b \tag{2}$$

Where M is the vehicle's mass, m is wheel's mass, F_b is the braking force, N is normal force from the ground, u is vehicle's forward velocity, ω_w is angular velocity of the wheel, J_w is wheel's moment of inertia, R_w is wheel's radius, τ_b is the brake torque. For the F_b , longitudinal tire force, we can write

$$F_b = \mu \cdot N \tag{3}$$

Where μ represents the longitudinal friction coefficient between the tire and the ground. There are different models for the tire forces such as Pacejka magic tire formula [5], Dugoff [6], LuGre [7], and Burckhardt [8]. In this paper, we choose a simplified Burckhardt model to represent the longitudinal tire model, for the sake of its simplicity and being able to capture longitudinal tire saturation well. The longitudinal friction coefficient is defined as

$$\mu = c_1 \cdot (1 - e^{-c_2 \lambda}) - c_3 \lambda \tag{4}$$

where c_1, c_2 and, c_3 are tire constants that depend on the road surface type (dry asphalt, wet asphalt, snow, ice) and λ is wheel slip and during the brake it is defined as

$$\lambda = \frac{u - R_w \omega_w}{u} \tag{5}$$

This relationship (Longitudinal friction Coefficient vs. Slip) is shown for a few of the road surfaces in Figure 2.

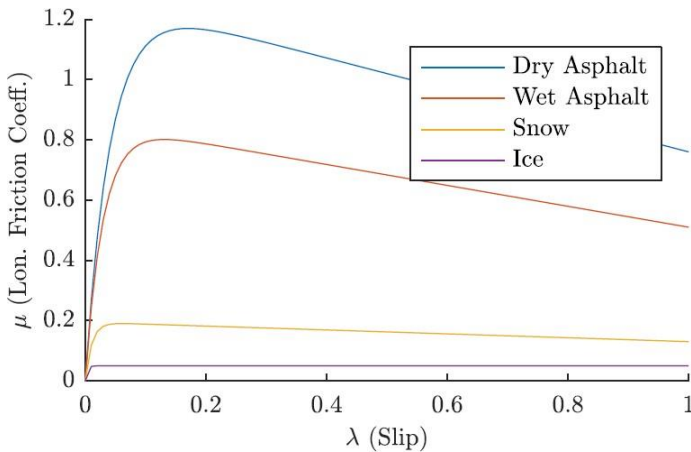


Figure 2: Longitudinal Friction Coefficient vs. Slip for different road surfaces using Burckhardt tire model

A brake actuator was also implemented similar to the one discussed in [9]. This actuator resembles the dynamics of an Electro-Hydraulic brake. The input to the system is the pressure input on the brake fluid lines and the output is the caliper position which then translates to the brake torque τ_b with the following equation

$$\tau_b = \begin{cases} 2\mu_{cal} r_{eff} k_{cal} (x_{cal} - x_0), & \text{if } x_{cal} \geq x_0 \\ 0, & \text{otherwise} \end{cases} \tag{6}$$

Where μ_{cal} , k_{cal} , r_{eff} , x_{cal} , and x_0 are the friction coefficient between the brake disk and caliper, brake pad stiffness, brake pad effective radius, caliper position, and the spacing between the brake pad and brake disk when there is no braking, respectively

Power Method

The overall control architecture of new continuous ABS algorithm method is shown in Figure 4. The main idea in this architecture lies under the "Power Method" block. It provides the brake torque reference to the control loop. Additionally, a low-level controller was designed for the brake system using Youla-Kucera robust control technique [4][10].

An overall schematic of the power method reference torque generator is given in Figure 3. The inputs to the Power Method reference generator are wheel angular velocity, the brake torque, and brake torque rate of change. The wheel angular velocity can be obtained through the wheel rate sensor. However, the brake torque is not readily available with the current sensors in a commercial vehicle. Therefore, estimation techniques can be utilized to obtain the estimated brake torque. The output of the reference generator is torque reference (τ_{ref}). We will discuss about ($\frac{d\tau}{dt}$) later in this section and also in the Mathematical Background section. Writing a simple power balance for the wheel yields to Equation 7.

$$\text{Power} = \dot{P}_w \omega + \tau_b \omega + F_b (u - R_{eff} \omega) = F_b u \tag{7}$$

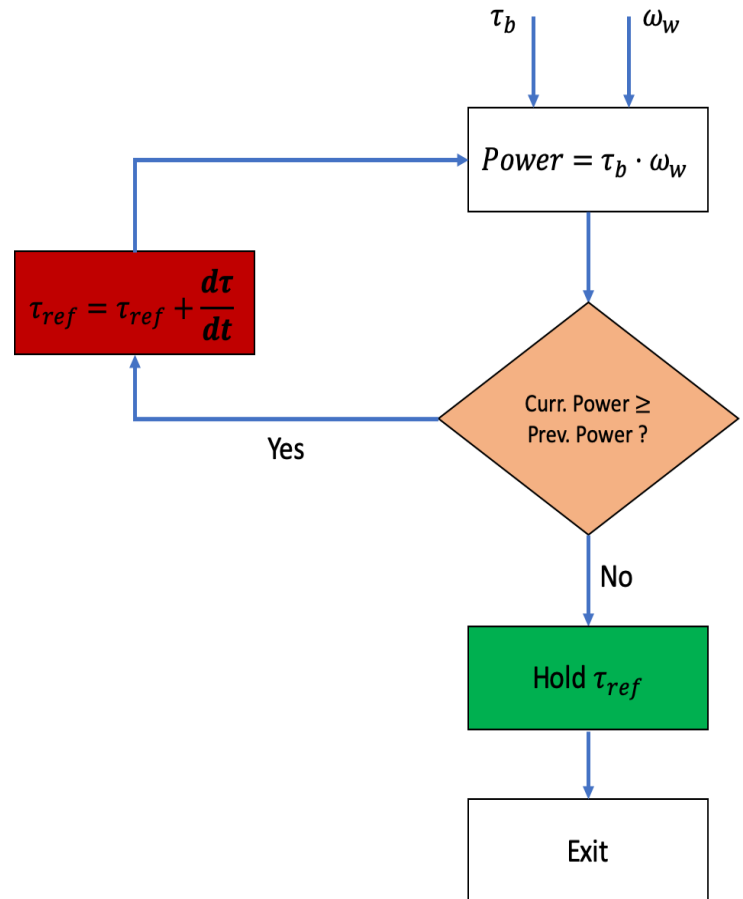


Figure 3: Power Method Reference Torque Generator for ABS

Where \dot{P}_ω , ω , r_b , F_b , u and R_{eff} are the derivative of angular momentum ($P_\omega = J_y \omega$, where J_y is wheel moment of inertia), wheel angular velocity, brake torque, brake force, vehicle speed and effective wheel radius, respectively. A steady state case is considered where there is no power exchange due to the tire inertia. This is a good approximation of operating in the linear region of the friction-slip curve where saturation momentum has less of an effect. Therefore, the power balance would result in Equation 8.

$$\text{Power dissipated} = \tau_b \omega = F_b R_{eff} \omega \quad (8)$$

Equation 8 shows that braking force of the vehicle is associated with the power dissipated by the brakes on wheel. If the power dissipated by the brakes is maximized, the braking force is also maximized. This happens near the peak of the friction-slip curve. If the slip becomes greater than the maximum slip, this will result in the wheel lock up (and therefore zero angular velocity of the wheel) and the power would immediately go to

zero. To search for maximizing the dissipation power, the algorithm shown in Figure 3 is used. It compares the previous power dissipation with the current power dissipation and if that power is increasing, then the dissipated power still has not reached its maximum. Therefore, the wheel torque brake can increase. Once the previous power dissipation is more than the current power dissipation, the maximum power dissipation has been reached and therefore, the previous brake torque is the maximum torque brake that can be exerted by the brake. Brake torque increase/decrease in each step is called $\frac{d\tau_b}{dt}$ (also referred as torque rate in this paper). This variable plays a very important rule in this heuristic search as we will discuss in the following sections. We will discuss different ways to find a solution for an optimal $\frac{d\tau_b}{dt}$ as it is a very important variable in the power method algorithm. Loyola et. al has suggested a 2-D lookup table based on acceleration and velocity of the vehicle for this variable. [4] In this paper, for more effectiveness and robustness of the method, we use an adaptive torque rate ($\frac{d\tau_b}{dt}$) during the ABS event.

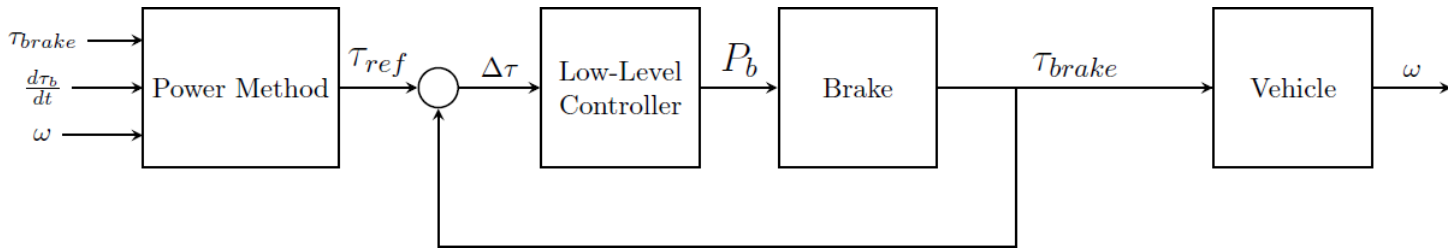


Figure 4: Overall control architecture of the new ABS method

Rate of Torque Calculation Using Coefficient of Friction

Linearizing the relationship between longitudinal force and longitudinal slip velocity requires,

$$F_b = \frac{\partial F_b}{\partial u_s} u_s + F_{b_0} \quad (9)$$

where u is the longitudinal slip velocity and is equal to

$$u_s = u - R_w \omega_w \quad (10)$$

And in the linear portion of the curve, $F_{b_0} = 0$. If we differentiate the wheel spin dynamics of Equation 1 with respect to time and substitute Equation 9; then we can write,

$$J_w \frac{d\dot{\omega}_w}{dt} = \frac{d}{dt} \left(\frac{\partial F_b}{\partial u_s} u_s R_w \right) - \frac{d\tau_b}{dt} \quad (11)$$

$$F_{b_{max}} = N \mu_{max} \quad (15)$$

Hence, we can simplify Equation 11 and approximate $\frac{d\tau_b}{dt}$ by the following equation,

$$\frac{d\tau_b}{dt} = N R_w \frac{\partial \mu(u_s)}{\partial u_s} \frac{du_s}{dt} \quad (12)$$

where in approximating Equation 11, we assumed that the angular jerk is relatively small compare to the other terms of Equation 11, the tire radius and $\frac{\partial F_b}{\partial u}$ are approximately constant and do not change with time, and $F_b = \mu N$, where N is the tire normal force and it is assumed that the normal force does not change with time (it has a slower dynamics than the wheel dynamics). Now, if we substitute Equation 5 into Equation 12 and replace $\dot{\omega}_m$ by its equivalent expression in 1, we can write,

$$\frac{1}{\frac{\partial \mu(u_s)}{\partial u_s}} \frac{dT_b}{dt} - \frac{N R_w^2}{J_w} T_b = N R_w \frac{du}{dt} - \frac{N R_w^3}{J_w} F_b \quad (13)$$

Equation 13 describes an approximate transient behavior of the tire with the longitudinal brake force as input and the brake torque as output. Furthermore, using Equation 2, we have

$$\frac{du}{dt} = -\frac{F_b}{M} \quad (14)$$

In addition, our search is for $F_{b_{max}}$ where,

We substitute Equation 14 and Equation 15 into the Equation 13, and we divide Equation 13 by $N R_w$, then we can write,

$$\frac{1}{\frac{\partial \mu(u_s)}{\partial u_s} N R_w} \frac{d\tau_b}{dt} = \frac{N R_w^2}{J_w} \frac{\tau_b}{N R_w} - \frac{N R_w^2}{J_w} \mu_{max} - \frac{N}{M} \mu_{max} \quad (16)$$

When working in the linear region of the longitudinal force vs. slip curve the term $\frac{cb}{NR_w}$ is equal to under the tire coefficient of friction μ . In addition, in Equation 16, the term $\frac{N}{M} \ll \frac{N}{J_w} \frac{2}{\omega}$; hence, we can ignore the term $\frac{N}{M} \mu_{max}$, and rewrite the Equation 16 as,

$$\frac{d\tau_b}{dt} = \alpha (\mu_{max} - \mu) \quad (17)$$

Where the proportionality constant is

$$\alpha = -\frac{\partial \mu(u_s)}{\partial u_s} \frac{R_w^3 N^2}{J_w} \quad (18)$$

Therefore, Equation 17 can be used for estimation of $\frac{dcb}{dt}$, provided an estimation of the road surface maximum coefficient of friction (μ_{max}) is available. As stated earlier, it is important to note by measuring the brake torque τ_b , and either computing or measuring the normal force N , it is then possible to compute the under tire coefficient of friction. Another important fact is that by having access to the road surface maximum coefficient of friction and the under tire coefficient of friction, it is possible to directly implement a force control strategy. This strategy simply minimizes the error between the under tire coefficient of friction and the road surface maximum coefficient of friction. Therefore, having the knowledge of μ_{max} and μ , an ABS controller would not be needed and can be replaced with a force control strategy. In the next subsection, we discuss a simpler method that does not require a knowledge of μ_{max} and lends itself very well in the power method brake torque generator for a continuous ABS.

Rate of Torque Calculation Using Longitudinal Tire Force

Assuming that ω_w is zero during the steady-state parts of the brake, from Equation 1, we can write

$$\tau_b = R_w \cdot F_b \quad (19)$$

Then $\frac{dcb}{dt}$ would become

$$\frac{d\tau_b}{dt} = R_w \cdot \frac{dF_b}{dt} \quad (20)$$

Which means that $\frac{dcb}{dt}$ can be calculated from the derivative of the tire longitudinal force. This would require an estimation of tire's longitudinal force which has been researched by many researchers such as [11],[12],[13],[14], and [15]. This force estimation along with the derivative would inherently add delays to this signal. Therefore, we have used a 10 milli-seconds delay for this signal.

In the next section, we present a few simulation results due to

implementation of the adaptive $\frac{dcb}{dt}$ power method using a rate of torque being calculated by the derivative of longitudinal tire force and its comparison with a constant rate of torque.

Results and Discussion

In this section, we discuss the results of the power method ABS algorithm which is proposed in the previous sections. The initial conditions for the simulations are different initial velocity of the vehicle, different road surfaces, and an initial slip which accounts for the time that ABS starts its process which is usually after moments of hard braking by the user. The initial slip is tested on different values (0.3 and 0.7) to ensure that the ABS power method algorithm works for initial slips near wheel lock ($\lambda = 1$) and smaller values which are still far from wheel lock. Figures 5, 6, 7, 8 and 9 show the results of the adaptive $\frac{dcb}{dt}$ using the derivative of longitudinal force. As shown in the Figures, this method performs well in different road surfaces, initial velocities, and initial slips. Figures 6 and 5 show the coefficient of friction ($\frac{F_b}{N}$) in different conditions. The maximum coefficient of friction is also plotted for the comparison. As shown in these figures, the vehicle is very close to the maximum friction coefficient without even getting near the locking of the wheel at any point (Figures 8 and 7). Figure 9 shows the reference brake torque generated using the power method at different speeds on a dry asphalt with the initial slip of 0.7. It takes longer for the algorithm to find the steady-state solution since at the higher velocities, the power dissipated would be larger; and therefore, the peak of the power happens later.

As seen in Figures 11 and 12, a constant $\frac{dc}{dt}$ can become sensitive over different conditions and will lock-up the wheel if this constant value is too high under certain road surfaces, initial velocities, and initial slips. And if the value of rate of torque is set low, it will result in a sub-optimal friction which would result in a longer stopping distance. Two different values of rate of torque has been tested and compared with the adaptive rate of torque which uses the derivative of longitudinal force. As shown in the Figures, this constant value is dependent on the road surface, initial velocity and initial slip that the ABS algorithm initiated which would require a look-up table and a lot of calibration and tuning during the implementation. In all the cases, the adaptive rate of torque shows a better performance (higher friction coefficient, μ) and does not lock the wheel. Figure 3 compares the dissipated power for to cases of constant rate of power and the adaptive rate of power for an initial velocity of 40 mph on a wet asphalt with the initial slip of 0.7. As we can see from Figure 11, when $\frac{dc}{dt} = 200$, the wheel locks up. This can be seen in Figure 3 as well since the dissipated power does not reach its peak and goes to zero before the other two cases. When $\frac{dc}{dt} = 200$, although it doesn't lock the wheel, and it looks like an optimal solution from a power point of view, the steady-state value of coefficient of friction doesn't stay close to the optimal solution and decreases. The only explanation for this would be that because of the nature of constant torque rate, once the algorithm reached one step before the peak of power (which would translate to the optimal brake torque), it then added one more constant step to the near optimal brake torque and it caused it to go over the peak of power; therefore, the coefficient of friction immediately dropped. This just proves what we discussed earlier regarding the constant rate of torque being hard to tune.

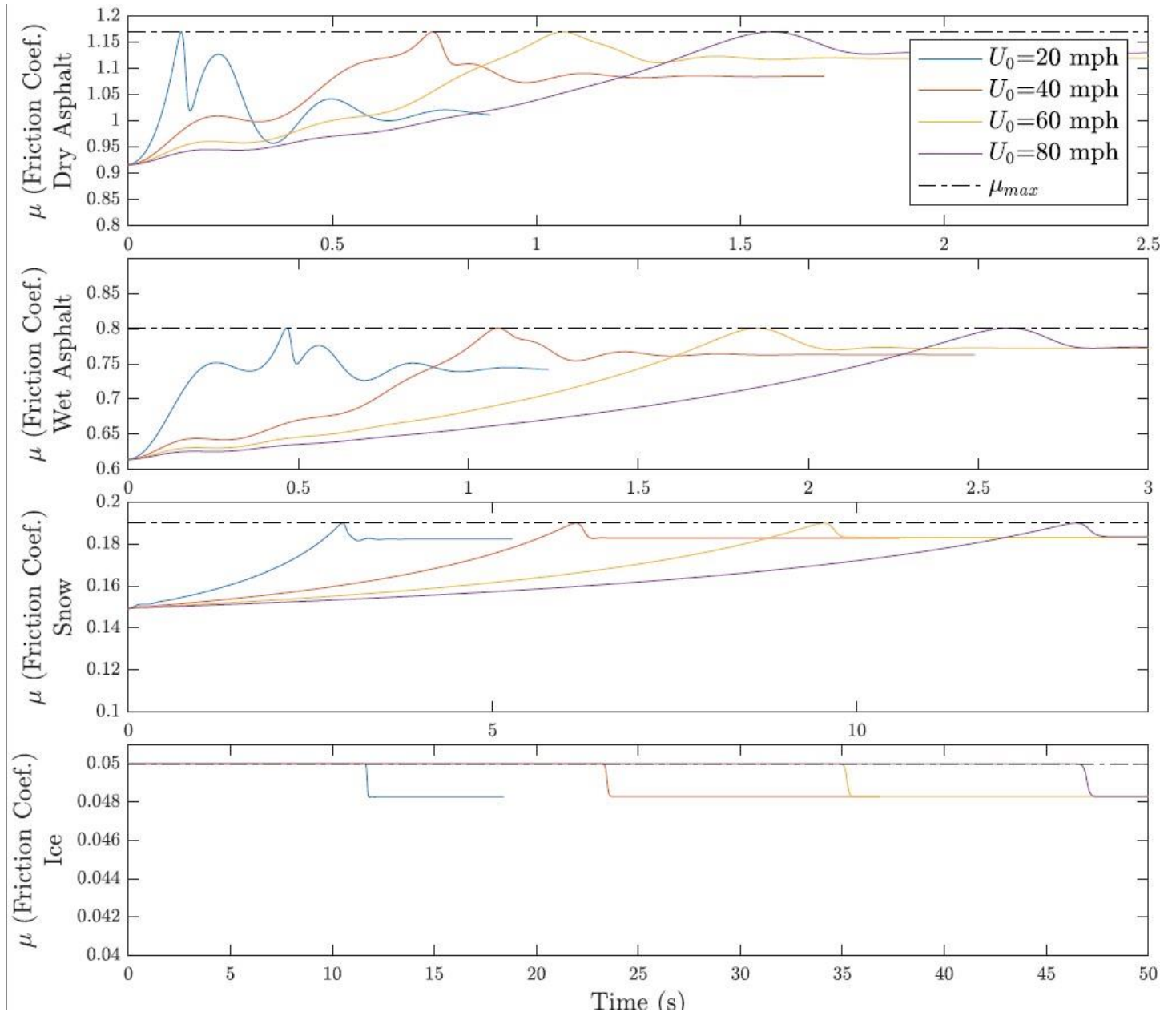


Figure 5: Coefficient of Friction vs. Time for various vehicle velocities (U_0) and road surfaces with the initial slip of $\lambda = 0.7$

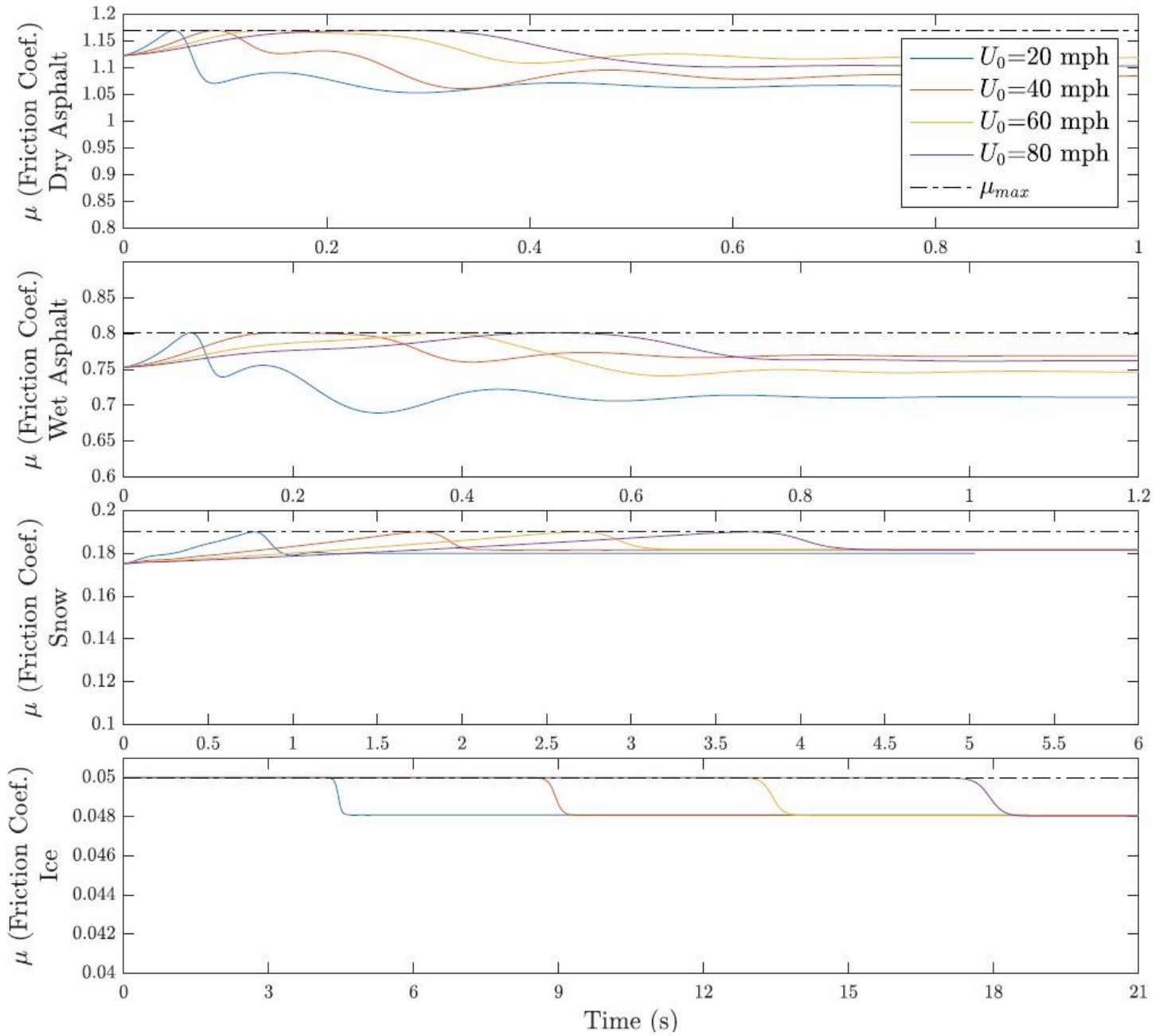


Figure 6: Coefficient of Friction vs. Time for various vehicle velocities (U_0) and road surfaces with the initial slip of $\lambda = 0.3$

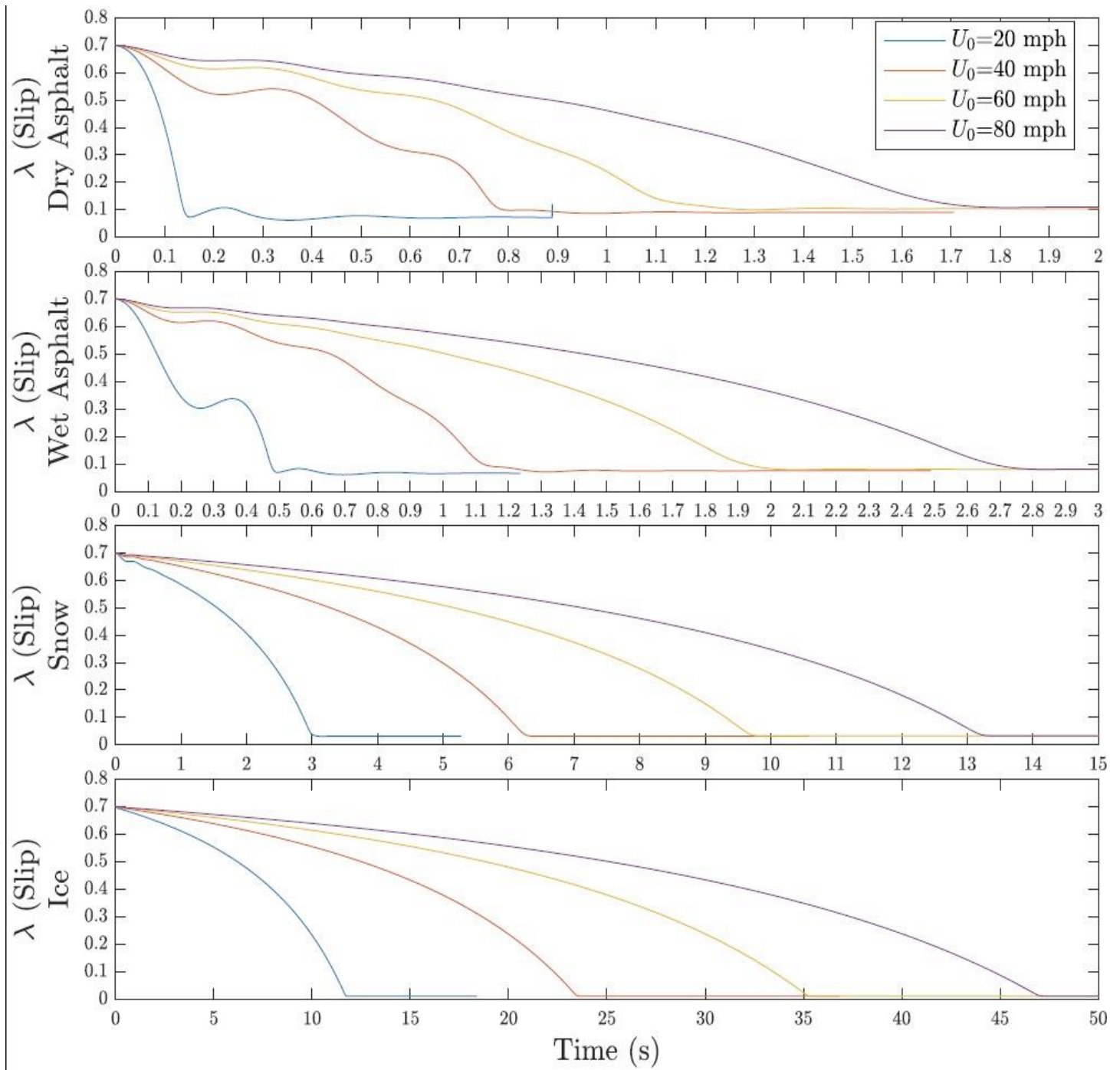


Figure 7: Slip vs. Time for various vehicle velocities (U_0) and road surfaces with the initial slip of $\lambda = 0.7$

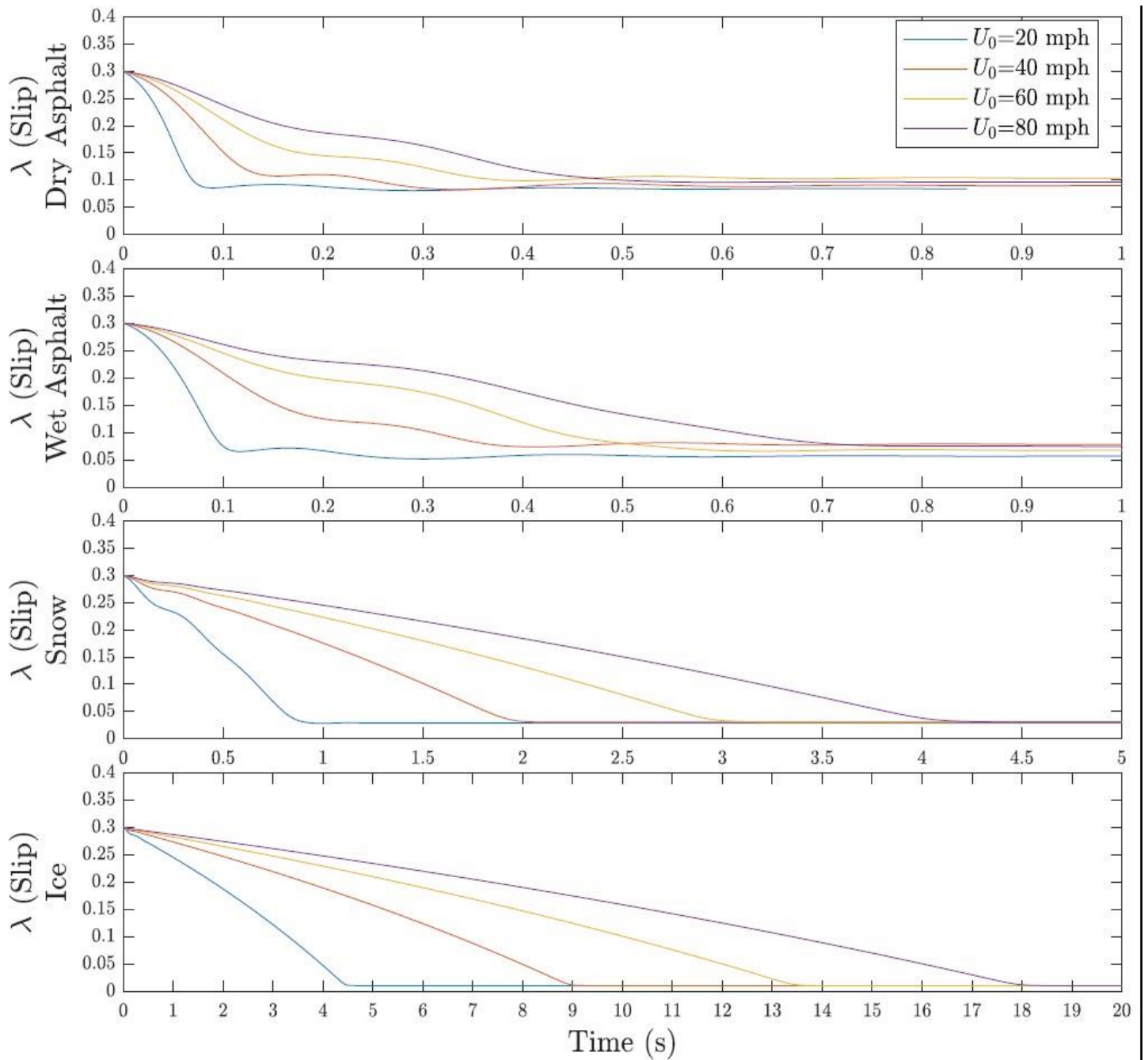


Figure 8: Slip vs. Time for various vehicle velocities (U_0) and road surfaces with the initial slip of $\lambda = 0.3$

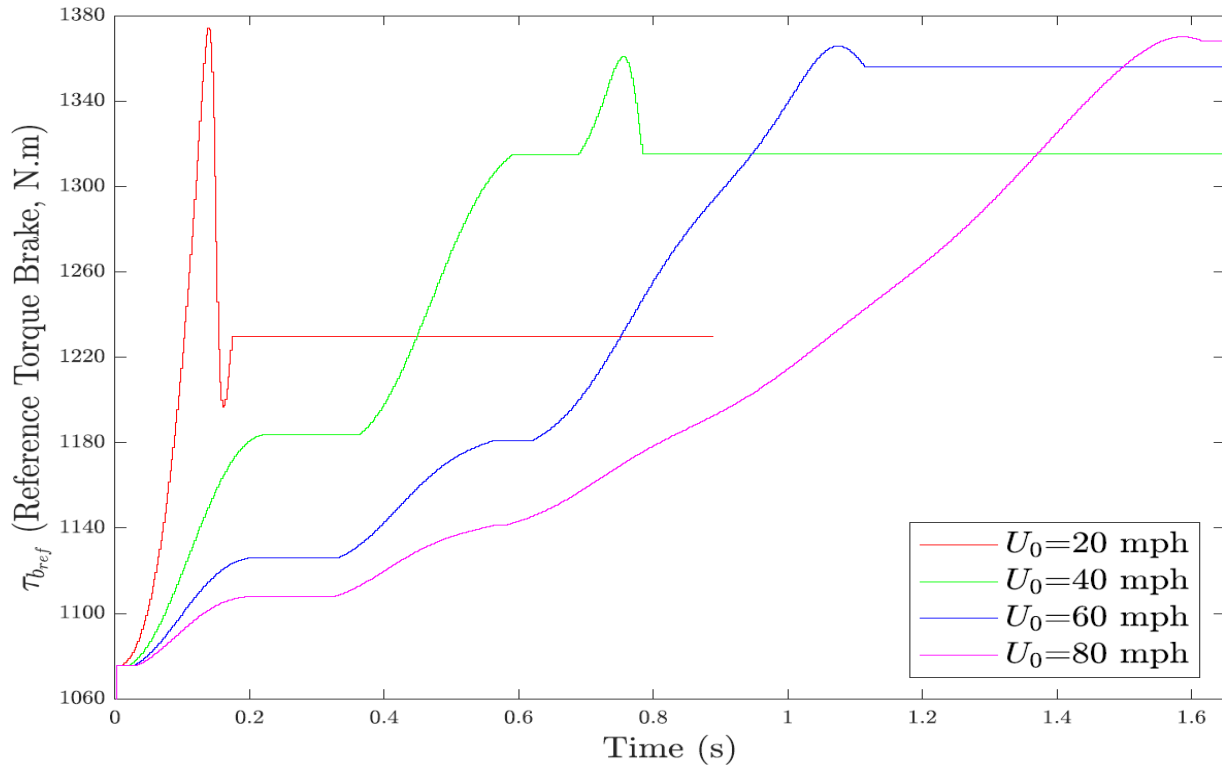


Figure 9: Reference Torque from Power Method vs. Time for various vehicle velocities (u_0) on a Dry Asphalt with the initial slip of $\lambda = 0.7$

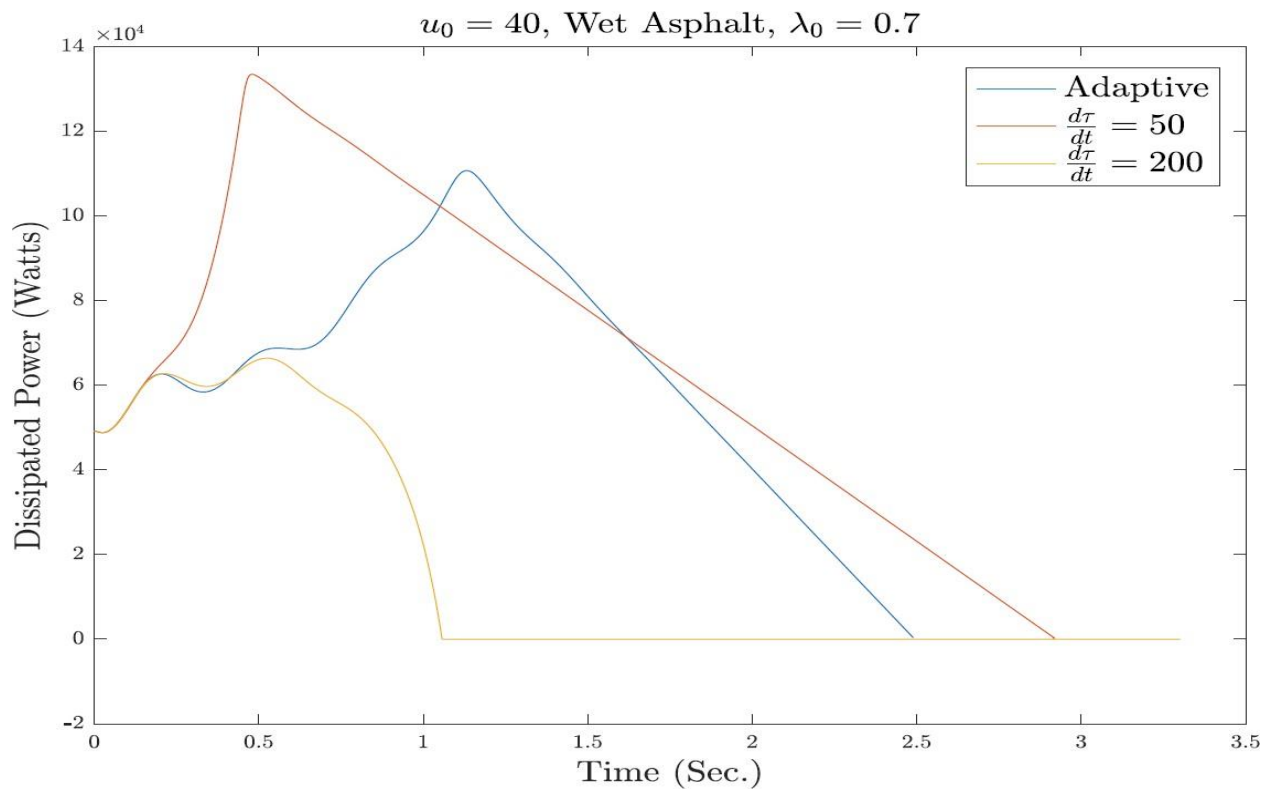


Figure 10: Comparison of constant $\frac{dC}{dt}$ vs. a variable $\frac{dC}{dt}$ - Dissipated Power vs. Time for initial velocity of 40 mph on a dry Asphalt and an initial slip of 0.7)

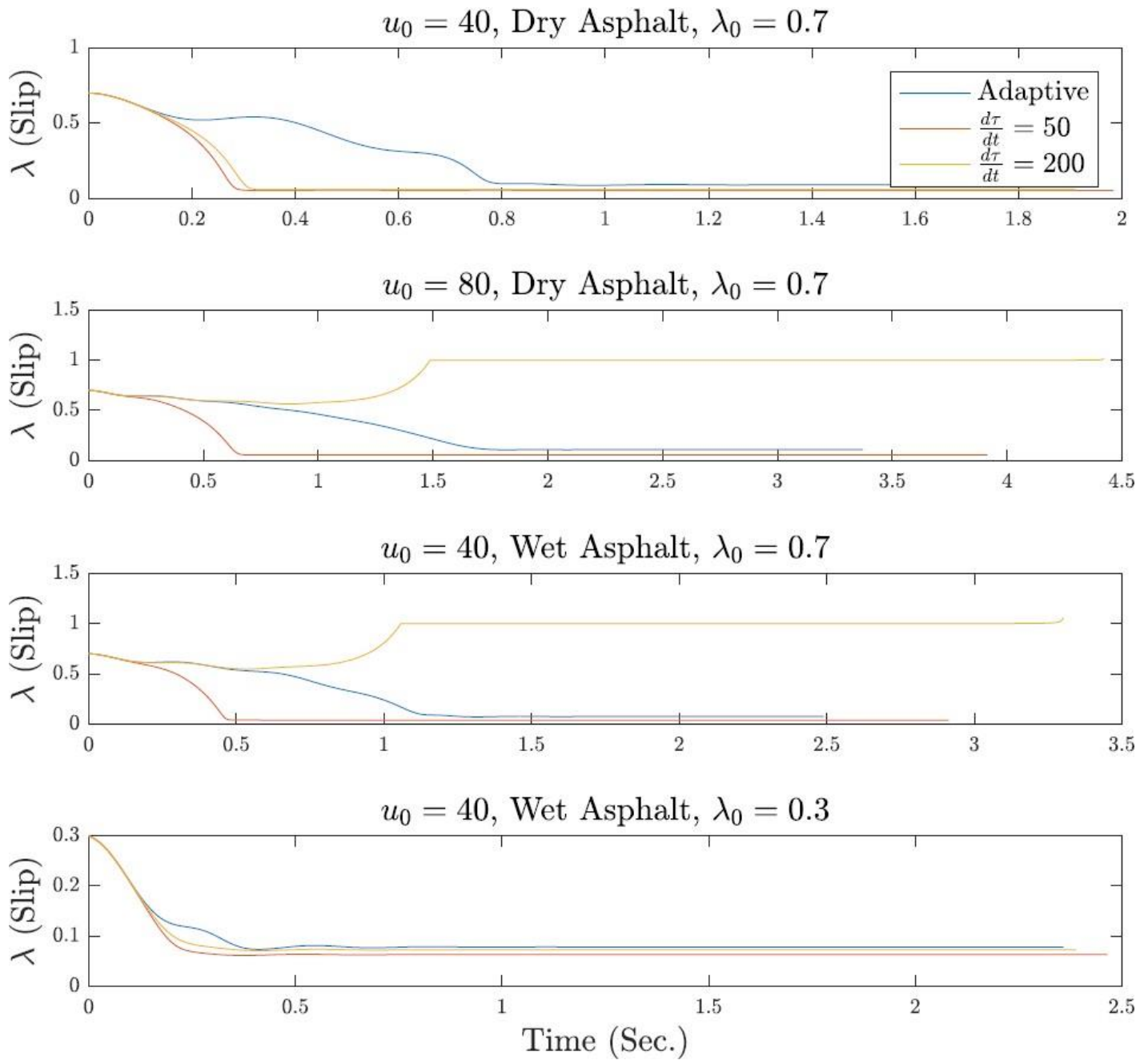


Figure 11: Comparison of constant $\frac{dc}{dt}$ vs. a variable $\frac{dc}{dt}$ - Slip vs. Time for various vehicle velocities (U_0), road surfaces and initial slips (λ_0)

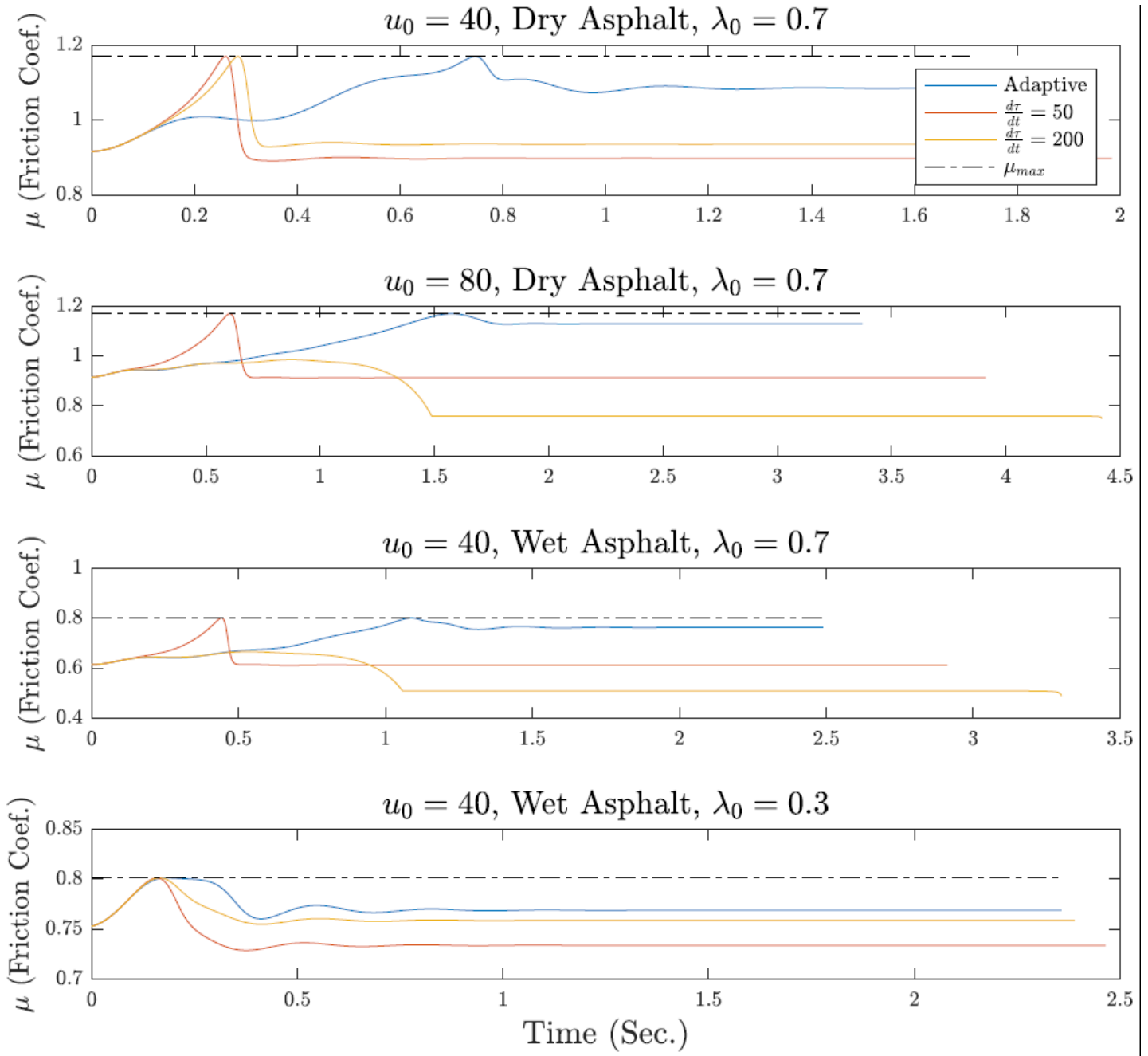


Figure 12: Comparison of constant $\frac{dc}{dt}$ vs. a variable $\frac{dc}{dt}$ - Coefficient of Friction vs. Time for various vehicle velocities (U_0), road surfaces and initial slips (λ_0)

Conclusion

We presented an ABS target generator using the dissipating power of the wheel for a continuous ABS control scheme. Different methods were used to find the a solution for a rate of torque that gives the best results. An adaptive rate of torque using the derivative of longitudinal force was used and showed promising results.

References

1. M.-c. Wu and M.-c. Shih, (2003) "Simulated and experimental study of hydraulic anti-lock braking system using sliding-mode pwm control," *Mechatronics*, vol. 13, no. 4, pp. 331–351,
2. D. Capra, E. Galvagno, V. Ondrak, B. Van Leeuwen, and A. Vigliani, (2012) "An abs control logic based on wheel force measurement," *Vehicle system dynamics*, vol. 50, no. 12, pp. 1779–1796,

3. F. Jiang and Z. Gao, (2000) "An adaptive nonlinear filter approach to the vehicle velocity estimation for abs," in *Proceedings of the 2000. IEEE International Conference on Control Applications. Conference Proceedings (Cat. No. 00CH37162)*, pp. 490–495, IEEE,
4. J. Loyola and F. Assadian, (2016) "An investigation into new abs control strategies," *SAE Int. J. Passeng. Cars - Mech. Syst.*, Apr.
5. H. B. Pacejka, *Tyre and Vehicle Dynamics*. Butterworth-Heinemann, 2012.
6. H. Dugoff, P. S. Fancher, and L. Segel, "An analysis of tire traction properties and their influence on vehicle dynamic performance," in *International Automobile Safety Conference*, SAE International, feb 1970.
7. C. C. De Wit, H. Olsson, K. J. Astrom, and P. Lischinsky, (1995) "A new model for control of systems with friction," *IEEE Transactions on automatic control*, vol. 40, no. 3, pp. 419–425,
8. M. Burckhardt, *Fahrwerktechnik: Radschlupf-Regelsysteme: Reifenverhalten, Zeitabläufe, Messung des Drehzustands der Raeder, Anti-Blockier-System (ABS), Theorie Hydraulikkreislaufe, Antriebs-Schlupf-Regelung (ASR), Theorie Hydraulikkreislaufe, elektronische Regeleinheiten, Leistungsgrenzen, ausgeführte Anti-Blockier-Systeme und Antriebs-Schlupf-Regelungen*. Vogel, 1993.
9. J. Loyola, "An investigation into new abs control strategies," Master's thesis, University of California, Davis,
10. V. Kučera, (2017) "A method to teach the parameterization of all stabilizing controllers," *IFAC Proceedings Volumes*, vol. 44, no. 1, pp. 6355–6360, 2011.
11. A. Rezaeian, R. Zarringhalam, S. Fallah, W. Melek, A. Khajepour, S.-K. Chen, N. Moshchuck, and B. Litkouhi, (2014) "Novel tire force estimation strategy for real-time implementation on vehicle applications," *IEEE Transactions on Vehicular Technology*, vol. 64, no. 6, pp. 2231–2241,
12. H. Hamann, J. K. Hedrick, S. Rhode, and F. Gauterin, (2014) "Tire force estimation for a passenger vehicle with the unscented kalman filter," in *2014 IEEE Intelligent Vehicles Symposium Proceedings*, pp. 814–819, IEEE,
13. L. R. Ray, (1997) "Nonlinear tire force estimation and road friction identification: simulation and experiments," *Automatica*, vol. 33, no. 10, pp. 1819–1833,
14. W. Cho, J. Yoon, S. Yim, B. Koo, and K. Yi, (2009) "Estimation of tire forces for application to vehicle stability control," *IEEE Transactions on Vehicular Technology*, vol. 59, no. 2, pp. 638–649,
15. J.V. Alcantar and F. Assadian, "Longitudinal tire force estimation using youla controller output observer," *IEEE Control Systems Letters*, vol. 2, no. 1, pp. 31–36, 2017.



This work is licensed under Creative Commons Attribution 4.0 License

To Submit Your Article Click Here: [Submit Manuscript](#)

DOI: [10.31579/JMAE.2020/002](https://doi.org/10.31579/JMAE.2020/002)

Ready to submit your research? Choose Auctores and benefit from:

- ❖ fast, convenient online submission
- ❖ rigorous peer review by experienced research in your field
- ❖ rapid publication on acceptance
- ❖ authors retain copyrights
- ❖ unique DOI for all articles
- ❖ immediate, unrestricted online access

At Auctores, research is always in progress.

Learn more www.auctoresonline.org/journals/journal-of-mechanical-and-aerospace-engineering